Glass forming tendency in ternary $Ge_xAs_{20}Te_{80-x}$ glasses examined using differential scanning calorimetry

2007 J. Phys.: Condens. Matter 19 096212

(http://iopscience.iop.org/0953-8984/19/9/096212)

IOP PUBLISHING JOURNAL OF PHYSICS: CONDENSED MATTER

J. Phys.: Condens. Matter **19** (2007) 096212 (11pp) doi:10.1088/0953-8984/19/9/096212

Glass forming tendency in ternary $Ge_xAs_{20}Te_{80-x}$ glasses examined using differential scanning calorimetry

E R Shaaban[1,3], **M T Dessouky**[2] **and A M Abousehly**[1]

[1] Department of Physics, Al-Azahar University, Assiut, 71542, Egypt
[2] Department of Physics, Al-Azahar University, Cairo, Egypt

E-mail: esam_ramadan2005@yahoo.com

Received 7 November 2006, in final form 22 January 2007
Published 14 February 2007
Online at stacks.iop.org/JPhysCM/19/096212

Abstract

The intermediate composition of $Ge_xAs_{20}Te_{80-x}$ glasses has been studied by differential scanning calorimetry. The intermediate glass formation and devitrification of $Ge_{10}As_{20}Te_{70}$ is proved more stable than the vicinity of intermediate compositions because the activation energy of transition, E_g (122.5 kcal mol^{-1}), of this composition shows a minimum at its average coordination number $r = 2.4$. The thermal stability of intermediate $Ge_{10}As_{20}Te_{70}$ glass is discussed based on characteristic temperatures such as the glass transition temperature, T_g, the crystallization temperature, T_p, and the melting temperature, T_m. The crystallization results are analysed and both the activation energy of the crystallization process ($E_c = 34.6$ kcal mol^{-1} for the first peaks and $E_c = 41.6$ kcal mol^{-1} for the second peaks) and the crystallization mechanism is characterized (kinetic exponent $n = 2.09$ for the first peaks, and $n = 1.02$ for the second peaks). The phases at which the alloy crystallizes after the thermal process have been identified by x-ray diffraction. The diffractogram of the transformed material indicates the presence of microcrystallites of $GeTe_4$ and AsTe, with an additional amorphous matrix remaining.

(Some figures in this article are in colour only in the electronic version)

1. Introduction

The glassy alloys of chalcogen elements were an initial object of study because of their interesting semiconducting properties [1, 2] and more recent importance in optical recording [3]. Recording materials must be stable in the amorphous state at low temperature

[3] Author to whom any correspondence should be addressed.

and have a short crystallization time. Promising materials with these characteristics have been recently studied [4]. Therefore, it is very important to know the glass forming ability and chemical durability of this type of materials. Recently, intermediate phases have been identified in chalcogenide glasses. These phases represent glass compositions where the glass forming tendency is optimized and ideal stress-free networks exist. In a region of optimal coordination ($r \sim 2.4$), glasses have been found to behave different from the expectation [5–9]. Glass compositions in this phase are quite stable. This is an area that has been steadily evolving [8, 9].

In the present work, both coordination number and activation energy of glass transition of $Ge_5As_{20}Te_{75}$, $Ge_{10}As_{20}Te_{70}$ and $Ge_{15}As_{20}Te_{65}$ are compared and it is proved that the composition $Ge_{10}As_{20}Te_{70}$ is more stable than the two other compositions. So the thermal stability of $Ge_{10}As_{20}Te_{70}$ glass has been discussed based on characteristic temperatures such as the glass transition temperature, T_g, the crystallization temperature, T_p, and the melting temperature, T_m. These thermal parameters are easily and accurately obtained by differential scanning calorimetry (DSC) during the heating processes of glassy alloy. Theoretical models [10–12] proposed for the crystallization process under non-isothermal conditions were applied to calculate crystallization kinetics. Finally, the crystalline phases corresponding to the crystallization process were identified by x-ray diffraction (XRD) measurements, using Cu Kα radiation.

2. Experimental details

The glassy alloys $Ge_5As_{20}Te_{75}$, $Ge_{10}As_{20}Te_{70}$ and $Ge_{15}As_{20}Te_{65}$ were made from their components of 99.999% purity. The proper amount for each material was weighed, and then the weighed materials were introduced into cleaned silica tubes. To avoid the oxidation of the samples the tubes were evacuated to 10^{-4} Pa. The ampoules were put into a furnace at around 1100 K for 24 h: hand shaking of the constituent materials inside the ampoule in the furnace was necessary to realize homogeneity of the composition; and then the ampoule was quenched in a water bath to avoid crystallization. The glassy nature of the material was confirmed through a diffractometric x-ray scan, in a Philips 1710 diffractometer, using Cu as target and Ni as filter ($\lambda = 1.542$ Å), showing an absence of the peaks which are characteristic of crystalline phases.

The calorimetric measurements were carried out using a Shimadzu 50 differential scanning calorimeter with an accuracy of ± 0.1 K. The calorimeter was calibrated, for each heating rate, using the well known melting temperatures and melting enthalpies of zinc and indium supplied with the instrument. 20 mg powdered samples were crimped into aluminium pans and scanned at continuous heating rates ($\beta = 5$, 10, 20, 30 and 40 K min^{-1}). The values of the glass transition, T_g, the crystallization extrapolated onset, T_c, and the crystallization peak, T_p, temperatures were determined with accuracy ± 1 K by using the microprocessor of the thermal analyser.

3. Average coordination number and thermal stability of intermediate compound

The average coordination number r in a ternary compound $Ge_xAs_yTe_z$ ($x + y + z = 1$) is calculated using the standard procedures described elsewhere [13, 9] as

$$r = x\mathrm{CN(Ge)} + y\mathrm{CN(As)} + z\mathrm{CN(Te)}. \quad (1)$$

Using coordination numbers (CNs) of 4, 3 and 2 for Ge, As and Te, respectively, the values of r of the $Ge_5As_{20}Te_{75}$, $Ge_{10}As_{20}Te_{70}$ and $Ge_{15}As_{20}Te_{65}$ glasses were evaluated; these values were 2.3, 2.4 and 2.5, respectively.

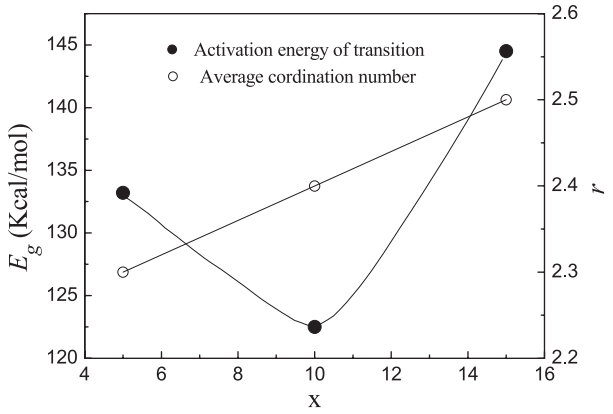

Figure 1. Activation energy of transition E_g and average coordination number r in $Ge_xAs_{20}Te_{80-x}$ glass alloys. As the predicted critical composition with $x = 10$ the E_g shows a minimum at $r = 2.4$.

The activation energies of glass transition E_g of three different compositions at different heating rates were calculated using Kissinger's formula [14], which will be defined later, when the glass transition is studied. The values of E_g were 133.2, 122.5 and 144.5 kcal mol^{-1} for three different compositions, respectively. The value of E_g (122.5 kcal mol^{-1}) shows a minimum at $r = 2.4$ for glass composition $Ge_{10}As_{20}Te_{70}$ (see figure 1); this indicates that this intermediate phase of glass composition is more stable than the two other intermediate phases [8, 9]. So we synthesize and analyse this intermediate bulk glass $Ge_{10}As_{20}Te_{70}$, because it may well be a good glass forming composition.

In order to evaluate the level of stability of the $Ge_{10}As_{20}Te_{70}$ glass, different simple quantitative methods have been suggested. Most of these methods [15–19] are based on characteristic temperatures such as the glass transition temperature, T_g, the crystallization temperature, T_p, and the melting temperature, T_m. These thermal parameters [20] are easily and accurately obtained by differential scanning calorimetry (DSC) during the heating processes of glass samples. The first thorough study on the glass thermal stability of various compounds was done by Sakka and Mackenzie [21], using the ratio T_g/T_m. Dietzel [15] introduced the glass criterion, $\Delta T = T_c - T_g$ (T_c is the onset temperature of crystallization), which is often an important parameter to evaluate the glass forming ability of the glasses. By the use of the characteristic temperatures, Hruby [9] developed the H_r criterion, $H_r = \Delta T/(T_m - T_p)$. Saad and Poulain obtained two criteria, weighted thermal stability H' and S criterion, $H' = \Delta T/T_g$, $S = (T_p - T_c)\Delta T/T_g$, respectively. In the present work, the above-mentioned criteria have been applied to the stable compound $Ge_{10}As_{20}Te_{70}$, and it is found that the parameters ΔT, H_r, H' and S increase with increasing heating rate, i.e. increasing in thermal stability (see table 1). In this table indices 1 and 2 to denote the first and second peaks respectively.

4. Results and discussion

In the present work, two exothermic overlapping peaks due to crystallization were observed at all different heating rates for $Ge_{10}As_{20}Te_{70}$ glass. Figure 2(a) shows the DSC traces for $Ge_{10}As_{20}Te_{70}$ glass at the two heating rates 5 and 40 K min^{-1}; this figure displays only one of the glass transition temperatures T_g for each rate; this figure also displays both the exothermic crystallization peaks and endothermic melting peaks, which consist of two overlapped peaks.

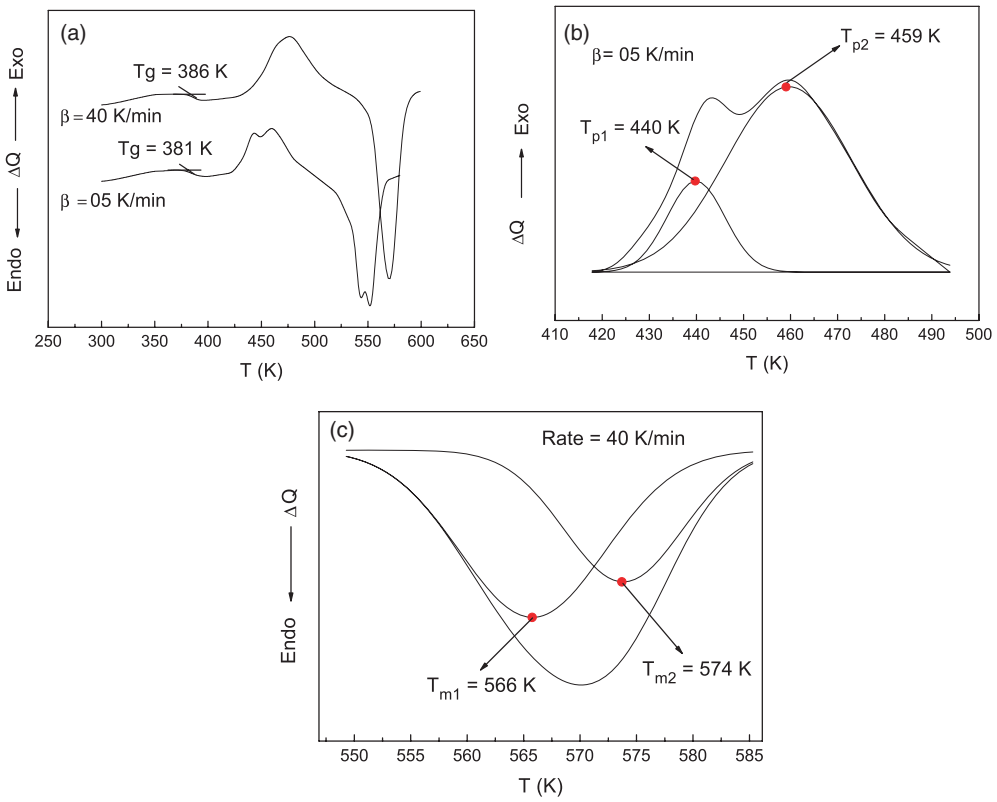

Figure 2. (a) Typical DSC trace of $Ge_{10}As_{20}Te_{70}$ glassy alloy at two heating rates, 5 and 40 K min^{-1}. (b) Separation of two overlapped crystallized peaks for heating rate 5 K min^{-1}; (c) separation of two overlapped melting peaks for heating rate 40 K min^{-1}.

Table 1. The values of thermal parameters of glass transition temperature T_g, onset temperature of crystallization T_c, crystallization temperature T_p and melting temperature T_m of $Ge_{10}As_{20}Te_{70}$ glass with different heating rates β. The characteristic parameters ΔT, H_r and S are according to the text. The indices 1 and 2 denote the first peaks and the second peaks respectively.

β	T_g	T_{c1}	T_{p1}	T_{m1}	ΔT_1	H_{r1}	S_1	T_{c2}	T_{p2}	T_{m2}	ΔT_2	H_{r2}	S_2
5	381	428.1	440	543	47.1	0.457	1.471	439	459	553	58	0.617	3.045
10	382.5	433.3	446	548	50.8	0.498	1.687	443	465	557	60.5	0.658	3.48
20	384	439.2	454	553	55.2	0.558	2.128	446	471	563	62	0.674	4.036
30	385	443.2	458	560	58.2	0.571	2.237	449	476	569	64	0.688	4.488
40	386	448.3	464	566	62.3	0.611	2.534	452	480	574	66	0.702	4.788

Figure 2(b) shows, for example, the separation of two overlapped crystallized peaks for heating rates of 5 K min^{-1}. Indices 1 and 2 in T_{p1} and T_{p2} denote the first peak and the second peak respectively. Figure 2(c) shows, for example, the separation of two overlapped melting peaks for heating rates 40 K min^{-1}, where T_{m1} and T_{m2} denote the first and the second peak.

Figure 3(a) shows that the fraction, χ, crystallized at a given temperature, T (for the first peak), is given by $\chi = A_T/A$, where A is the total area of the exothermic peak between the temperature, T_I, where crystallization is just beginning and the temperature, T_f, where the crystallization is completed; A_T is the area between T_I and T.

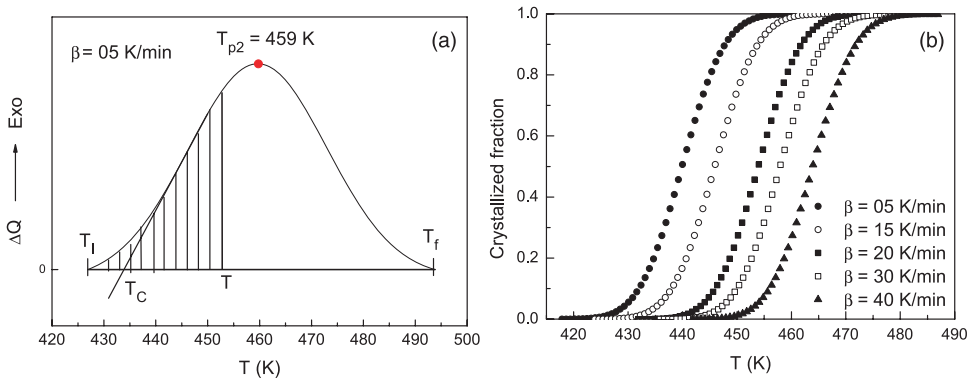

Figure 3. (a) Exothermic second peak of rate 5 K min^{-1}; the line area A_T is shown between T_I and T_f of the peak; T_I, T_f and T according to the text; (b) crystallized fraction as a function of temperature at different heating rates for first crystallization curves.

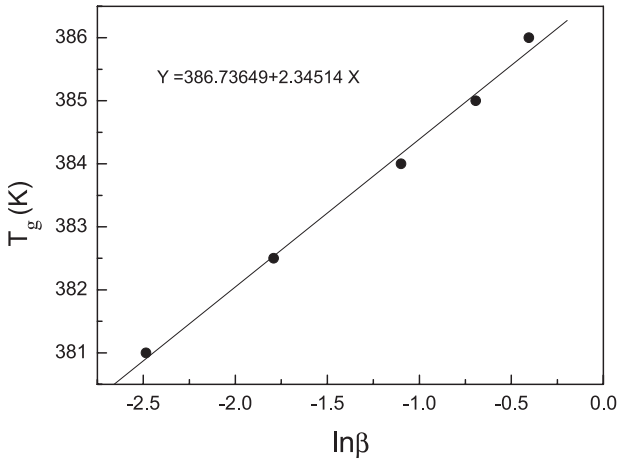

Figure 4. Glass transition temperature T_g versus ln β (β in K s^{-1}) of $Ge_{10}As_{20}Te_{70}$, glass.

The presence of two peaks means that there are two phases appearing during the crystallization process. The phases in which the alloy crystallizes after the thermal process have been identified by x-ray diffraction.

The graphical representation of the volume fraction crystallized shows the typical sigmoid curve as a function of temperature for different heating rates' first crystallization curves (see figure 3(b)) in crystallization reactions, as it appears in the literature [2, 22].

4.1. Glass transition

Two approaches are used to analyse the dependence of T_g on the heating rate. One is the empirical relationship of the form $T_g = A + B \ln \beta$, where A and B are constants for a given glass composition [23]. For the $Ge_{10}As_{20}Te_{70}$ glass, the empirical relationship can be written as $T_g = 386.7 + 2.35 \ln(\beta)$, where a straight regression line has been fitted to the experimental data; see figure 4.

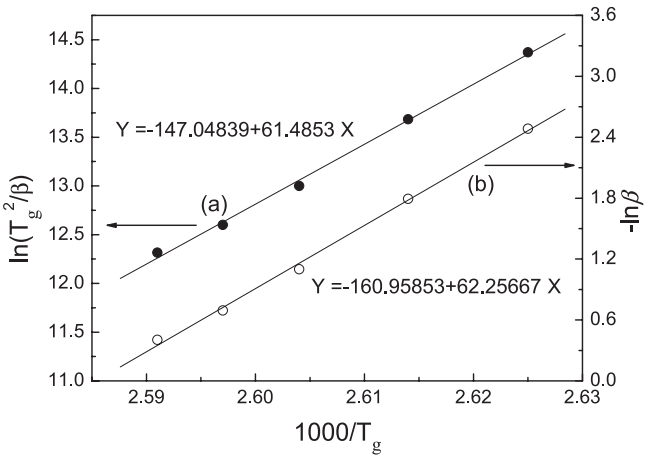

Figure 5. (a) Plot of $\ln T_g^2/\beta$ versus $1000/T_g$ of the analysed material. (b) Plot of $\ln\beta$ versus $1000/T_g$ of the studied glass β in K s^{-1}.

The other approach is the dependence of the glass transition temperature on heating rate β, by using Kissinger's formula [14] in the form [24, 25]

$$\ln(T_g^2/\beta) = E_g/RT_g + \text{const} \tag{2}$$

a straight line between $\ln(T_g^2/\beta)$ and $1/T_g$, whose slope yields a value of E_g, where the subscript g denotes magnitude values corresponding to the glass transition temperature. In addition, if it is assumed that, usually, the change in $\ln T_g^2$ with β is negligibly small compared with the change in $\ln\beta$ [26], one obtains

$$\ln(\beta) = -E_g/RT_g + \text{const}, \tag{3}$$

a straight line, whose slope also yields a value of E_g.

Figure 5 shows the plots of $\ln(T_g^2/\beta)$ (a) and $\ln(\beta)$ (b) versus $1/T_g$ for the $Ge_{10}As_{20}Te_{70}$ glass, displaying the linearity of the equations used. The values of the activation energy obtained for the glass transition are 122.5 ± 2 kcal mol^{-1} (plot (a)) and 124 ± 2 kcal mol^{-1} (plot (b)), respectively.

4.2. Crystallization

The theoretical basis for interpreting DSC results is provided by the formal theory of transformation kinetics as developed by Johnson and Mehl [27] and Avrami [28, 29]. The ratio between the ordinates of the DSC curve and the total area of the peak gives the corresponding crystallization rates, which makes it possible to build the curves of the exothermal peaks represented in figure 6(a). It may be observed that the $(dx/dt)_p$ values increase as well as the heating rate, a property which has been widely discussed in the literature [30]. From the experimental values of $(dx/dt)_p$ one can calculate the kinetic exponent n by using the following equation:

$$(d\chi/dt)_p = n(0.37\beta E_c)/(RT_p^2). \tag{4}$$

The n values for $Ge_{10}As_{20}Te_{70}$ glass are calculated and listed in table 2.

For the evaluation of activation energy for crystallization (E_c) by using the variation of T_p with β, Vázquez *et al* [25] developed a method for non-isothermal analysis of devitrification as

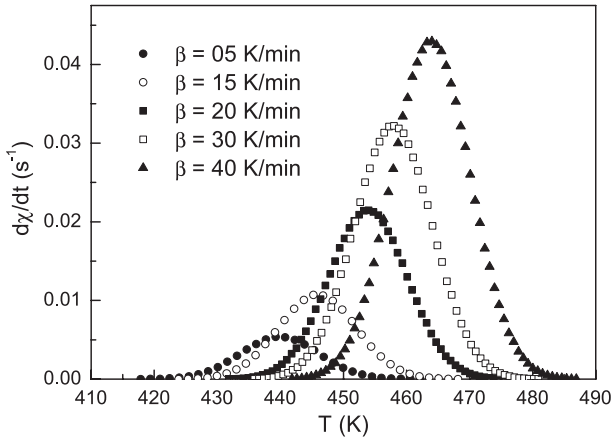

Figure 6. (a) Crystallization rate versus temperature of the exothermal peaks at different heating rates for the first peaks.

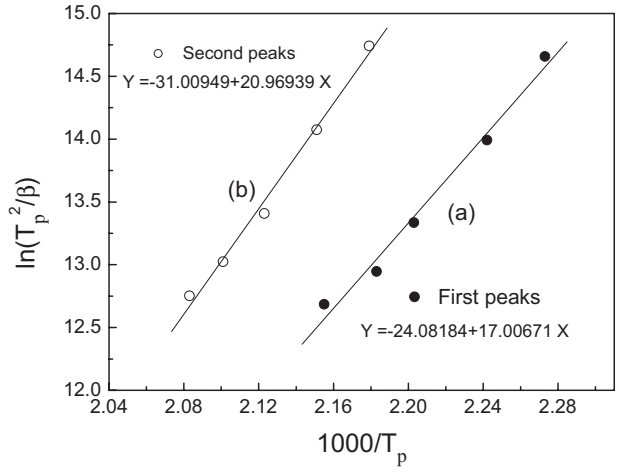

Figure 7. Experimental plot of $\ln T_p^2/\beta$ versus $1000/T_p$ (for both two separated peaks (a) and (b)) straight regression lines of $Ge_{10}As_{20}Te_{70}$, alloy (β in K s^{-1}).

Table 2. Maximum crystallization rate ($d\chi/dt$), kinetic exponent n and average kinetic exponent $\langle n \rangle$ for the different heating rates β. The indices 1 and 2 denote the first peaks and the second peaks respectively.

β	$(d\chi/dt)_1$ (s^{-1})	n_1	$\langle n_1 \rangle$	$(d\chi/dt)_2$ (s^{-1})	n_2	$\langle n_2 \rangle$
5	0.0054	1.987		0.0029	0.939	
10	0.011	2.023		0.0061	1.013	
20	0.021	2.106	2.09	0.012	1.039	1.02
30	0.032	2.139		0.0182	1.038	
40	0.043	2.194		0.0241	1.066	

follows:

$$\ln[T_p^2/\beta] = E_c/RT_p + \ln q \tag{5}$$

where q is the pre-exponential factor. From the experimental data a plot of $\ln(T_p^2/\beta)$ versus

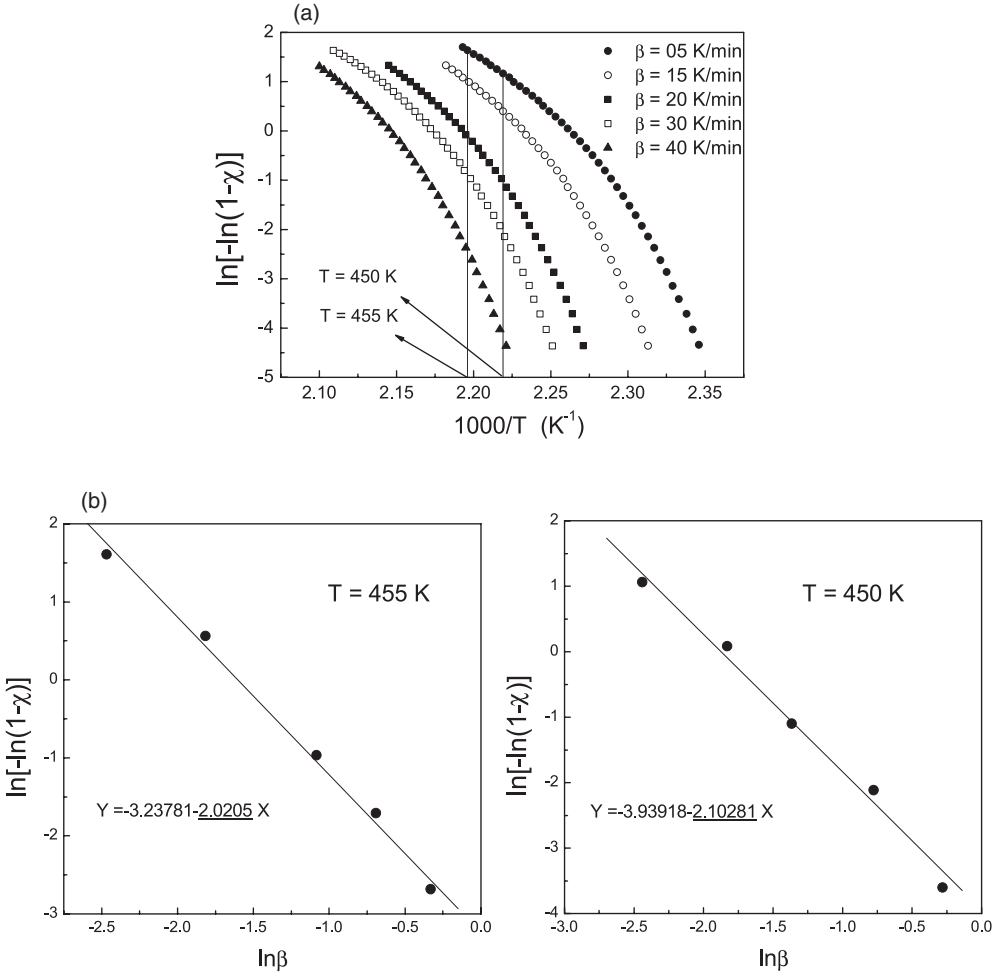

Figure 8. (a) Plot of $\ln[-\ln(1-\chi)]$ versus $1000/T$ for the first exothermic peak at different heating rates. (b) Plot of $\ln[-\ln(1-\chi)]$ versus $\ln\beta$ for the first exothermic peak at two different temperatures. (The underlined value is the Avrami index.)

$1/T_p$ has been drawn at each heating rate, and also the straight regression line shown in figures 7(a) and (b) for each peak. From the slope of this experimental straight line it is possible to deduce the value of the activation energy, $E_c = 34.6 \pm 1.0$ kcal mol^{-1}, for the first peaks and $E_c = 41.6 \pm 1.0$ kcal mol^{-1} for the second peaks and for the crystallization process, and the origin ordinate gives the value corresponding to the logarithm of the pre-exponential factor, $\ln q = 24.1$ for the first peaks and 31 for the second peaks (q in (K s)$^{-1}$).

Finally, the experimental data, T_p, and $(dx/dt)_p$, shown in tables 1 and 2 respectively, and the above mentioned value of the activation energies of the crystallization process for two peaks, make it possible to determine, through relationship (4), the kinetic exponent, n, for each of the experimental heating rates for two groups of peaks, whose values are also given in table 2, the mean value being $\langle n \rangle = 2.09$ for the first peaks and 1.02 for the second peaks. Allowing for experimental error, the value of $\langle n \rangle$ is close to two for the first phase and close to unity for the second phase. The kinetic exponent was deduced based on the mechanism of

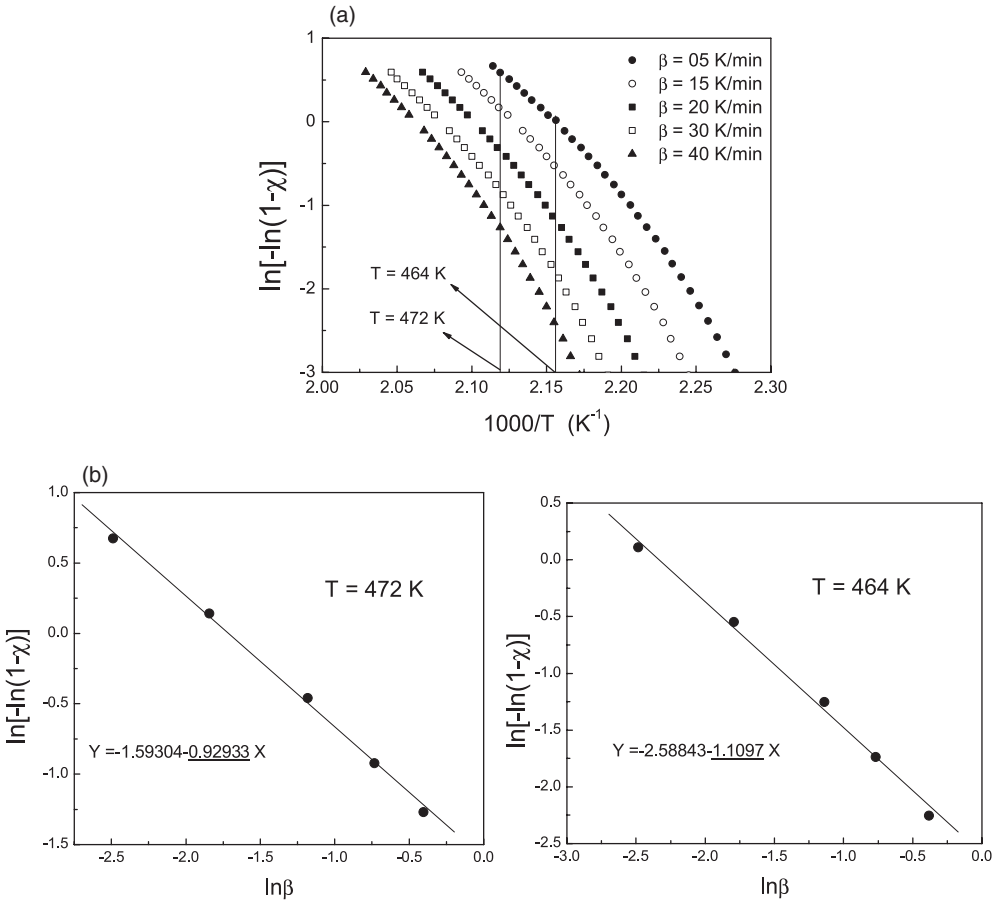

Figure 9. (a) Plot of $\ln[-\ln(1-\chi)]$ versus $1000/T$ for the second exothermic peak at different heating rates. (The underlined value is the Avrami index.) (b) Plot of $\ln[-\ln(1-\chi)]$ versus $\ln\beta$ for the second exothermic peak at two different temperatures. (The underlined value is the Avrami index.)

crystallization [31]. The $\langle n\rangle$ value of the kinetic exponent of the as-quenched glass is consistent with the mechanism of volume nucleation with two-dimensional growth for the first phase and one-dimensional growth for the second phase [31].

In the non-isothermal crystallization, the volume fraction of crystallites, χ, precipitated in a glass heated at constant rate, β, is related to the crystallization activation energy, E_c, through the following expression [32]:

$$\ln[-\ln(1-\chi)] = -n\ln\beta - 1.052(mE/RT) + \text{const} \tag{6}$$

where m and n are integers or half-integers which depend on the mechanism of the growth and the dimensionality of the crystal [33]. Besides, from the mean value of the kinetic exponent, n, it is possible to postulate a crystallization reaction mechanism for the $Ge_{10}As_{20}Te_{70}$ glassy alloy. Mahadevan *et al* [34] have shown that n may be 4, 3 or 2, which are related to different glass–crystal transformation mechanisms: $n = 4$, volume nucleation, three-dimensional growth; $n = 3$, volume nucleation, two-dimensional growth, $n = 2$, volume nucleation, one-dimensional growth; $n = 1$, surface nucleation, one-dimensional growth from surface to the

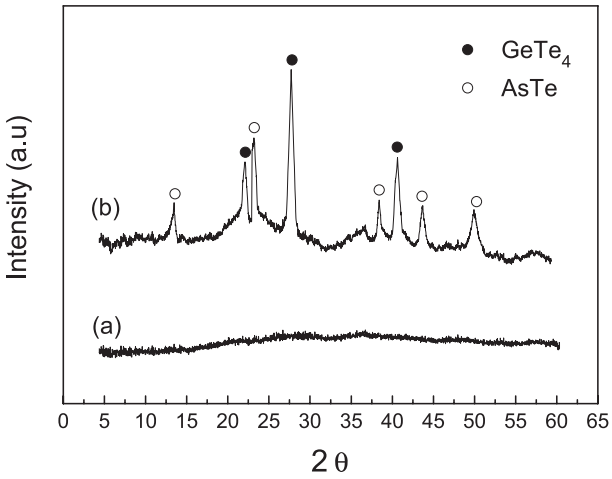

Figure 10. (a) Diffractogram of glassy alloy of $Ge_{10}As_{20}Te_{70}$. (b) Diffraction peaks of the alloy after thermal treatment (annealing at 475 K for 2 h).

inside. Therefore, bearing in mind the above obtained mean value, $n = 2.09$ for the first peaks means volume nucleation, one-dimensional growth, and $n = 1.02$ for the second peaks means surface nucleation, one-dimensional growth from surface to the inside.

The kinetic parameter n, for both the crystallization exotherms, can also be calculated using equation (6) by plotting $\ln[-\ln(1-\chi)]$ versus $1/T$ for all the heating rates (figures 8(a) and 9(a)). From the data obtained from figures 8(a) and 9(a), a plot of $\ln[-\ln(1-\chi)]$ versus $\ln\beta$ at constant temperature can be performed. Figures 8(b) and 9(b) show the relation between $\ln[-\ln(1-\chi)]$ and $\ln\beta$ at two fixed temperatures for both the crystallization exotherms. From the slope of this relation one can deduce the order of the crystallization mechanism (or Avrami index), n. Allowing for experimental error, the value of $\langle n\rangle$ is close to two for the first phase and close to unity for the second phase. This confirms the value of n calculated from equation (4).

5. Identification of the crystalline phases

To identify the possible phases that crystallize during the thermal treatment applied to the samples, we examine the x-ray diffraction patterns of glassy alloy $Ge_{10}As_{20}Te_{70}$, annealed at 475 K for 2 h. For this purpose, figure 10 shows the most relevant portions of the diffractometer tracings for the as quenched glass and for the material subjected to the thermal process. Figure 10(a), characteristic of the amorphous phase of the starting material, has been measured at diffraction angles (2θ) between 4° and 60°. The diffractogram of the transformed material after the crystallization process suggests the presence of microcrystallites of two phases. From the JCPDS files these peaks can be identified as $GeTe_4$ (card No 33-0585) and AsTe (card No 37-1125) crystalline phases as shown in figure 10(b), which were the cause of the presence of two peaks overlapped in the DSC traces for $Ge_{10}As_{20}Te_{70}$ glass at different heating rates. No presence of Te was observed in the XRD pattern, maybe due to the fact that Te still remains in the amorphous phase.

6. Conclusion

The intermediate phase of $Ge_{10}As_{20}Te_{70}$ is more stable compared to other vicinity intermediate phases of $Ge_5As_{20}Te_{75}$ and $Ge_{15}As_{20}Te_{65}$. So crystallization of a $Ge_{10}As_{20}Te_{70}$ glass sample

has been studied using calorimetric and x-ray powder diffraction techniques. The study of crystallization kinetics was performed using the formal theory of transformations for heterogeneous nucleation. The kinetic parameters, activation energy of the glass transition, activation energy for the crystallization process, kinetic exponent n and exponential factor have been deduced depending on the heating rate. In addition, two approaches have been used to analyse the glass transition. One is the linear dependence of the glass transition temperature on the logarithm of the heating rate. The other is the linear relationship between the logarithm of the quotient (T_g^2/β) and the reciprocal of the glass transition temperature. Finally, recording the x-ray diffraction pattern of the transformed material enabled identification of the crystalline phases. This pattern shows the existence of microcrystallites of $GeTe_4$ and AsTe in an amorphous matrix, while there remains also a residual amorphous phase.

Acknowledgment

The authors are grateful to Al-Azhar University Faculty of Science Physics Department Assuit branch for financial support.

References

[1] Tanaka K, Osaka Y, Sugi M, Iizima S and Kikuchi M 1973 *J. Non-Cryst. Solids* **12** 100
[2] Shaaban E R 2006 *Physica* B **373** 211
[3] Sugiyama Y, Chiba R, Fugimori S and Funakoski N 1990 *J. Non-Cryst. Solids* **122** 83
[4] Fugimori S, Sagi S, Yamazaki H and Funakoski N 1988 *J. Appl. Phys.* **64** 100
[5] Boolchand P, Georgiev D G and Micoulaut M 2002 *J. Optoelectron. Adv. Mater.* **4** 823
[6] Chakravarty S, Georgiev D G, Boolchand P and Micoulaut M 2005 *J. Phys.: Condens. Matter* **17** L1
[7] Georgiev D G, Boolchand P and Micoulaut M 2000 *Phys. Rev.* B **62** R9228
[8] Boolchand P, Lucovsky G, Philips J C and Thorpe M F 2005 *Phil. Mag.* **85** 3823
[9] Wang F, Mamedov S, Boolchand P, Goodman B and Chandrasekhar M 2005 *Phys. Rev.* B **71** 174201
[10] Matusita K, Konatsu T and Yokota R 1984 *J. Mater. Sci.* **19** 291
[11] Vazquez J, Lopez-Alemany P L, Villares P and Jimenez-Garay R 2000 *J. Phys. Chem. Solids* **61** 493
[12] Strink M J and Zahra A M 1997 *Thermochim. Acta* **298** 179
[13] Loffe A F and Regel A R 1960 *Prog. Semicond.* **4** 239
[14] Kissinger H E 1956 *J. Res. Nat. Bur. Stand.* **57** 217
[15] Dietzel A 1968 *Glastech. Ber.* **22** 41
[16] Uhlmann D R 1972 *J. Non-Cryst. Solids* **7** 337
[17] Uhlmann D R 1977 *J. Non-Cryst. Solids* **25** 43
[18] Hruby A 1972 *Czech. J. Phys.* B **22** 1187
[19] Saad M and Poulain M 1987 *Mater. Sci. Forum* **19/20** 11
[20] Malek J 1988 *J. Non-Cryst. Solids* **107** 323
[21] Sakka S and Mackenzie J D 1971 *J. Non-Cryst. Solids* **6** 145
[22] Wagner C, Villanes P, Vázquez J and Jirnénexz-Caray R R 1993 *Mater. Lett.* **19** 370
[23] Lasocka -M 1976 *Mater. Sci. Eng.* **23** 173
[24] Chen H S 1978 *J. Non-Cryst. Solids* **27** 257
[25] Vázquez J, Wagner C, Villares P and Jiménez Garay R 1998 *J. Non-Cryst. Solids* **235–237** 548
[26] Sestak J 1974 *Phys. Chem. Glasses* **15** 137
[27] Johnson W A and Mehl R F 1939 *Trans. Am. Inst. Min. Met. Eng.* **135** 416
[28] Avrami M 1940 *J. Chem. Phys.* **8** 212
[29] Avrami M 1941 *J. Chem. Phys.* **9** 177
[30] Gao Y Q, Wang W, Zheng F Q and Liu X 1986 *J. Non-Cryst. Solids* **81** 135
[31] Matusita K and Saka S 1980 *J. Non-Cryst. Solids* **38/39** 741
[32] Matusita K, Konatsu T and Yorota R 1984 *J. Mater. Sci.* **19** 291
[33] Yinnon H and Uhlmann D R 1983 *J. Non-Cryst. Solids* **54** 253
[34] Mahadevan S, Giridhar A and Sing A K 1986 *J. Non-Cryst. Solids* **88** 11